Computational Fluid and Solid Mechanics

Series Editor:

Klaus-Jürgen Bathe
Massachusetts Institute of Technology
Cambridge, MA, USA

Advisors:

Franco Brezzi
University of Pavia
Pavia, Italy

Olivier Pironneau
Université Pierre et Marie Curie
Paris, France

Available Volumes

D. Chapelle, K.J. Bathe
The Finite Element Analysis of Shells – Fundamentals
2003

D. Drikakis, W. Rider
High-Resolution Methods for Incompressible and Low-Speed Flows
2005

M. Kojic, K.J. Bathe
Inelastic Analysis of Solids and Structures
2005

E.N. Dvorkin, M.B. Goldschmit
Nonlinear Continua
2005

B.Q. Li
Discontinuous Finite Elements in Fluid Dynamics and Heat Transfer
2006

J. Iannelli
Characteristics Finite Element Methods in Computational Fluid Dynamics
2006

S. Gopalakrishnan, A. Chakraborty, D. Roy Mahapatra
Spectral Finite Element Method
2007

S. Gopalakrishnan • A. Chakraborty
D. Roy Mahapatra

Spectral Finite Element Method

Wave Propagation, Diagnostics and Control in Anisotropic and Inhomogeneous Structures

Springer

Authors

S. Gopalakrishnan, PhD
Department of Aerospace Engineering
Indian Institute of Science
C.V Raman Avenue
Bangalore 560 012
India

A. Chakraborty, PhD
General Motors India
Units 1–8, 3rd Floor, Creator Building
Whitefield Road
Bangalore 560 066
India

D. Roy Mahapatra, PhD
Department of Aerospace Engineering
Indian Institute of Science
C.V Raman Avenue
Bangalore 560 012
India

ISBN 978-1-84628-355-0 e-ISBN 978-1-84628-356-7

DOI 10.1007/978-1-84628-356-7

Computational Fluid and Solid Mechanics Series ISSN 1860-482X

British Library Cataloguing in Publication Data
A catalogue record for this book is available from the British Library

Library of Congress Control Number: 2007938275

Cover design: deblik, Berlin, Germany

Printed on acid-free paper

9 8 7 6 5 4 3 2 1

springer.com

To our parents and wives

Preface

Wave propagation is an exciting field having applications cutting across many disciplines. In the field of structural engineering and smart structures, wave propagation based tools have found increasing applications especially in the area of structural health monitoring and active control of vibrations and noise. In addition, there has been tremendous progress in the area of material science, wherein a new class of structural materials is designed to meet the particular application. In most cases, these materials are not isotropic as in metallic structures. They are either anisotropic (as in the case of laminated composite structures) or inhomogeneous (as in the case of functionally graded materials). Analysis of these structures is many orders more complex than that of isotropic structures. For many scientists/engineers, a clear difference between structural dynamics and wave propagation is not evident. Traditionally, a structural designer will not be interested in the behavior of structures beyond certain frequencies, which are essentially at the lower end of the frequency scale. For such situations, available general purpose finite element code will satisfy the designer's requirement. However, currently, structures are required to be designed to sustain very complex and harsh loading environments. These loadings are essentially multi-modal phenomena and their analysis falls under the domain of wave propagation rather than structural dynamics. Evaluation of the structural integrity of anisotropic and inhomogeneous structures subjected to such loadings is a complex process. The currently available analysis tools are highly inadequate to handle the modeling of these structures. In this book, we present a technique called the "Spectral Finite Element Method", which we believe will address some of the shortcomings of the existing analysis tools.

Although the spectral finite element method has been in existence for a long time under the name of the dynamic stiffness method, its use was limited to simple vibration studies. It is only in recent times that the potential of this method to handle a wide range of applications has been realized. This is evident from the increasing number of publications in the archival literature. However, we believe that its impact has reached only a small subset

of scientists/engineers working in these areas due to the non-availability of a good textbook. The main aim of this book is to reach out to those analysts/engineers working in new and cutting edge areas to not only highlight the power of this method, but also to serve as a good reference book for specialists.

The spectral finite element method is essentially a finite element method in the frequency domain. In essence, the beauty of the method lies in the fact that one can easily convert a finite element code to a spectral element code without much difficulty. In addition, it uses spectral analysis as a basic tool for element formulation. That is, in the process of element formulation, one can deeply understand the physics behind wave propagation in complex media and its interaction with various boundaries. Frequency domain formulation enables easy and straightforward solution of inverse problems. Hence, the spectral element method can be used as a tool to post-process experimental data.

The book mainly addresses the wave behavior in composites and inhomogeneous media in addition to its application to structural health monitoring and active vibration and wave control. The book introduces new methods for the solution of wavenumbers for propagation in composites and inhomogeneous waveguides. For structural health monitoring, waveguide models for different types of damage are developed. The reader is also introduced to various damage detection schemes that blend well with the spectral element method. Towards the end of the book, a chapter on the use of the spectral element method for active control application is presented.

A step by step modular approach is adopted here in writing this book. A number of numerical results are presented to not only emphasize the efficiency and numerical superiority of the method, but also to bring out the physics of the problem. The reader may notice that in most cases only one element is sufficient for solution of certain problems, where thousands of finite elements are required. The material presented in this book can serve as a graduate level textbook on wave propagation in structures. A separate graduate level course on the spectral finite element method can be developed using this book. This book is written assuming that the reader has only an elementary background in the theory of elasticity, strength of materials, linear algebra and methods for solving ordinary and partial differential equations.

We would like to thank many of the graduate students who have contributed directly or indirectly towards the development of the book. We would particularly thank A. Nag, D. Srikanth, A. Garg and A. Singhal for their contributions.

Bangalore, India
October, 2007

S. Gopalakrishnan
A. Chakraborty
D. RoyMahapatra

Contents

1 Introduction 1
1.1 Solution Methods for Wave Propagation Problems 1
1.2 Fourier Analysis 6
1.2.1 Continuous Fourier Transforms 6
1.2.2 Fourier Series 9
1.2.3 Discrete Fourier Transform 11
1.3 Spectral Analysis 15
1.4 What is the Spectral Element Method? 19
1.5 Outline and Scope of Book 21

2 Introduction to the Theory of Anisotropic and Inhomogeneous Materials 23
2.1 Introduction to Composite Materials 23
2.2 Theory of Laminated Composites 24
2.2.1 Micromechanical Analysis of a Lamina 25
2.2.2 Strength of Materials Approach to Determination of Elastic Moduli 25
2.2.3 Stress–Strain Relations for a Lamina 29
2.2.4 Stress–Strain Relation for a Lamina with Arbitrary Orientation of Fibers 31
2.3 Introduction to Smart Composites 34
2.4 Modeling Inhomogeneous Materials 38

3 Idealization of Wave Propagation and Solution Techniques . 41
3.1 General Form of the Wave Equations 41
3.2 Characteristics of Waves in Anisotropic Media 42
3.3 General Form of Inhomogeneous Wave Equations 43
3.4 Basic Properties and Solution Techniques 43
3.5 Spectral Finite Element Discretization 44
3.6 Efficient Computation of the Wavenumber and Wave Amplitude 48

3.6.1 Method 1: The Companion Matrix and the SVD Technique 49
3.6.2 Method 2: Linearization of PEP 50
3.7 Spectral Element Formulation for Isotropic Material 51
3.7.1 Spectral Element for Rods 51
3.7.2 Spectral Element for Beams 53

4 Wave Propagation in One-dimensional Anisotropic Structures 55
4.1 Wave Propagation in Laminated Composite Thin Rods and Beams 55
4.1.1 Governing Equations and PEP 56
4.1.2 Spectrum and Dispersion Relations 58
4.2 Spectral Element Formulation 59
4.2.1 Finite Length Element 59
4.2.2 Throw-off Element 61
4.3 Numerical Results and Discussions 61
4.3.1 Impact on a Cantilever Beam 61
4.3.2 Effect of the Axial–Flexural Coupling 63
4.3.3 Wave Transmission and Scattering Through an Angle-joint 66
4.4 Wave Propagation in Laminated Composite Thick Beams: Poisson's Contraction and Shear Deformation Models 69
4.4.1 Wave Motion in a Thick Composite Beam 70
4.4.2 Coupled Axial–Flexural Shear and Thickness Contractional Modes 72
4.4.3 Correction Factors at High Frequency Limit 74
4.4.4 Coupled Axial–Flexural Shear Without the Thickness Contractional Modes 76
4.4.5 Modeling Spatially Distributed Dynamic Loads 79
4.5 Modeling Damping Using Spectral Element 81
4.5.1 Proportional Damping Through a Discretized Finite Element Model 81
4.5.2 Proportional Damping Through the Wave Equation . . . 83
4.6 Numerical Results and Discussions 88
4.6.1 Comparison of Response with Standard FEM 91
4.6.2 Presence of Axial–Flexural Shear Coupling 93
4.6.3 Parametric Studies on a Cantilever Beam 96
4.6.4 Response of a Beam with Ply-drops 96
4.7 Layered Composite Thin-walled Tubes 99
4.7.1 Linear Wave Motion in Composite Tube 102
4.8 Spectral Finite Element Model 107
4.8.1 Short and Long Wavelength Limits for Thin Shell and Limitations of the Proposed Model 107
4.8.2 Comparison with Analytical Solution 114

4.9 Numerical Simulations 116
4.9.1 Time Response Under Short Impulse Load and the Effect of Fiber Orientations 116

5 Wave Propagation in One-dimensional Inhomogeneous Structures 123
5.1 Length-wise Functionally Graded Rod 124
5.1.1 Development of Spectral Finite Elements 126
5.1.2 Smoothing of Reflected Pulse 132
5.2 Depth-wise Functionally Graded Beam 135
5.2.1 Spectral Finite Element Formulation 137
5.2.2 The Spectrum and Dispersion Relation 137
5.2.3 Effect of Gradation on the Cut-off Frequencies 139
5.2.4 Computation of the Temperature Field 142
5.3 Wave Propagation Analysis: Depth-wise Graded Beam (HMT) 142
5.3.1 Validation of the Formulated SFE 143
5.3.2 Lamb Wave Propagation in FSDT and HMT Beams . . 148
5.3.3 Effect of Gradation on Stress Waves 151
5.3.4 Coupled Thermoelastic Wave Propagation 153
5.4 Length-wise Graded Beam: FSDT 157
5.4.1 Spectral Finite Element Formulation 158
5.4.2 Effect of Gradation on the Spectrum and Dispersion Relation 159
5.4.3 Effect of Gradation on the Cut-off Frequencies 160
5.5 Numerical Examples 162
5.5.1 Effect of the Inhomogeneity 162
5.5.2 Elimination of the Reflection from Material Boundary . . 165

6 Wave Propagation in Two-dimensional Anisotropic Structures 171
6.1 Two-dimensional Initial Boundary Value Problem 172
6.2 Spectral Element for Doubly Bounded Media 176
6.2.1 Finite Layer Element (FLE) 177
6.2.2 Infinite Layer Element (ILE) 178
6.2.3 Expressions for Stresses and Strains 178
6.2.4 Prescription of Boundary Conditions 179
6.2.5 Determination of Lamb Wave Modes 179
6.3 Numerical Examples 181
6.3.1 Propagation of Surface and Interface Waves 181
6.3.2 Propagation of Lamb Wave 185

7 Wave Propagation in Two-dimensional Inhomogeneous Structures 195
7.1 SLE Formulation: Inhomogeneous Media 195
7.1.1 Exact Formulation 196

7.2 Numerical Examples 201
7.2.1 Propagation of Stress Waves 201
7.2.2 Propagation of Lamb Waves 204
7.3 SLE Formulation: Thermoelastic Analysis 208
7.3.1 Inhomogeneous Anisotropic Material 209
7.3.2 Discussion on the Properties of Wavenumbers 212
7.3.3 Finite Layer Element (FLE) 215
7.3.4 Infinite Layer Element (ILE) 216
7.3.5 Homogeneous Anisotropic Material 217
7.4 Numerical Examples 217
7.4.1 Effect of the Relaxation Parameters - Symmetric Ply-layup 217
7.4.2 Interfacial Waves: Thermal and Mechanical Loading . . . 220
7.4.3 Propagation of Stress Waves 221
7.4.4 Propagation of Thermal Waves 226
7.4.5 Effect of Inhomogeneity 227
7.5 Wave Motion in Anisotropic and Inhomogeneous Plate 229
7.5.1 SPE Formulation: CLPT 230
7.5.2 Computation of Wavenumber: Anisotropic Plate 234
7.5.3 Computation of Wavenumber: Inhomogeneous Plate . . . 237
7.5.4 The Finite Plate Element 241
7.5.5 Semi-infinite or Throw-off Plate Element 242
7.6 Numerical Examples 243
7.6.1 Wave Propagation in Plate with Ply-drop 243
7.6.2 Propagation of Lamb waves 246

8 Solution of Inverse Problems: Source and System Identification 249
8.1 Force Identification 249
8.1.1 Force Reconstruction from Truncated Response 250
8.2 Material Property Identification 253
8.2.1 Estimation of Material Properties: Inhomogeneous Layer 254

9 Application of SFEM to SHM: Simplified Damage Models . 259
9.1 Various Damage Identification Techniques 259
9.1.1 Techniques for Modeling Delamination 260
9.1.2 Modeling Issues in Structural Health Monitoring 261
9.2 Modeling Wave Scattering due to Multiple Delaminations and Inclusions 262
9.3 Spectral Element with Embedded Delamination 265
9.3.1 Modeling Distributed Contact Between Delaminated Surfaces 269
9.4 Numerical Studies on Wave Scattering due to Single Delamination 271
9.4.1 Comparison with 2-D FEM 271

9.4.2 Identification of Delamination Location from Scattered Wave . . . 273
9.4.3 Effect of Delamination at Ply-drops . . . 274
9.4.4 Sensitivity of the Delaminated Configuration . . . 276
9.5 A Sublaminate-wise Constant Shear Kinematics Model . . . 279
9.6 Spectral Elements with Embedded Transverse Crack . . . 284
9.6.1 Element-internal Discretization and Kinematic Assumptions . . . 284
9.6.2 Modeling Dynamic Contact Between Crack Surfaces . . . 288
9.6.3 Modeling Surface-breaking Cracks . . . 290
9.6.4 Distributed Constraints at the Interfaces Between Sublaminates and Hanging Laminates . . . 291
9.7 Numerical Simulations . . . 293
9.7.1 Comparison with 2-D FEM . . . 293
9.7.2 Identification of Crack Location from Scattered Wave . . . 294
9.7.3 Sensitivity of the Crack Configuration . . . 296
9.8 Spectral Finite Element Model for Damage Estimation . . . 297
9.8.1 Spectral Element with Embedded Degraded Zone . . . 300
9.9 Numerical Simulations . . . 301

10 Application of SFEM to SHM: Efficient Damage Detection Techniques . . . 307
10.1 Strategies for Identification of Damage in Composites . . . 307
10.2 Spectral Power Flow . . . 311
10.2.1 Properties of Spectral Power . . . 312
10.2.2 Measurement of Wave Scattering due to Delaminations and Inclusions Using Spectral Power . . . 314
10.3 Power Flow Studies on Wave Scattering . . . 314
10.3.1 Wave Scattering due to Single Delamination . . . 314
10.3.2 Wave Scattering due to Length-wise Multiple Delaminations . . . 316
10.3.3 Wave Scattering due to Depth-wise Multiple Delaminations . . . 317
10.4 Wave Scattering due to Strip Inclusion . . . 319
10.4.1 Power Flow in a Semi-infinite Strip Inclusion with Bounded Media: Effect of Change in the Material Properties . . . 319
10.4.2 Effect of Change in the Material Properties of a Strip Inclusion . . . 321
10.5 Damage Force Indicator for SFEM . . . 323
10.6 Numerical Simulation of Global Identification Process . . . 327
10.6.1 Effect of Single Delamination . . . 327
10.6.2 Effect of Multiple Delaminations . . . 329
10.6.3 Sensitivity of Damage Force Indicator due to Variation in Delamination Size . . . 330

10.6.4 Sensitivity of Damage Force Indicator due to Variation in Delamination Depth . . . 331
10.7 Genetic Algorithm (GA) for Delamination Identification . . . 337
10.7.1 Objective Functions in GA for Delamination Identification . . . 338
10.7.2 Displacement-based Objective Functions . . . 338
10.7.3 Power-based Objective Functions . . . 343
10.8 Case Studies with a Cantilever Beam . . . 346
10.8.1 Identification of Delamination Location . . . 346
10.8.2 Identification of Delamination Size . . . 348
10.8.3 Identification of Delamination Location and Size . . . 349
10.8.4 Identification of Delamination Location, Size and Depth 349
10.8.5 Effect of Delamination Near the Boundary . . . 350
10.9 Neural Network Integrated with SFEM . . . 352
10.10 Numerical Results and Discussion . . . 357

11 Spectral Finite Element Method for Active Wave Control . 365
11.1 Challenges in Designing Active Broadband Control Systems . . 365
11.1.1 Strategies for Vibration and Wave Control . . . 366
11.1.2 Active LAC of Structural Waves . . . 371
11.2 Externally Mounted Passive/Active Devices . . . 372
11.3 Modeling Distributed Transducer Devices . . . 377
11.3.1 Plane Stress Constitutive Model of Stacked and Layered Piezoelectric Composite . . . 378
11.3.2 Constitutive Model for Piezoelectric Fiber Composite (PFC) . . . 381
11.3.3 Design Steps for Broadband Control . . . 391
11.4 Active Spectral Finite Element Model . . . 394
11.4.1 Spectral Element for Finite Beams . . . 394
11.4.2 Sensor Element . . . 395
11.4.3 Actuator Element . . . 395
11.4.4 Numerical Implementation . . . 397
11.5 Effect of Broadband Distributed Actuator Dynamics . . . 398
11.6 Active Control of Multiple Waves in Helicopter Gearbox Support Struts . . . 402
11.6.1 Active Strut System . . . 404
11.6.2 Numerical Simulations . . . 405
11.7 Optimal Control Based on ASFEM and Power Flow . . . 415
11.7.1 Linear Quadratic Optimal Control Using Spectral Power 416
11.7.2 Broadband Control of a Three-member Composite Beam Network . . . 417

References . . . 423

Index . . . 439

1

Introduction

Dynamic analysis in structural engineering falls into two different classes, one involving low frequency loading and the other involving high frequency loading. Low frequency problems are categorized as ***Structural Dynamics*** problems while those involving high frequency loading fall into the category of ***Wave Propagation*** problems. In structural dynamics problems, the frequency content of the dynamic load is of the order of a few hundred hertz (Hz) and the designer will be mostly interested in the long-term (or steady-state) effects of the dynamic load on the structures. Hence, the first few normal modes and natural frequencies are sufficient to assess the performance of the structure. The phase information of the response is not critical here. Most of the dynamic problems in structures will fall into this category. On the other hand, for wave propagation problems, the frequency content of the input loading is very high (of the order of kilohertz (kHz) or higher) and hence, short-term effects (transient response) become very critical. Further, many higher order modes will participate in amplifying the dynamic response. Impact and blast-type of loading fall into this category. The multi-modal nature of wave propagation makes one parameter very important, and that is the phase information.

1.1 Solution Methods for Wave Propagation Problems

Dynamic analyses are traditionally performed using the conventional Finite Element Method (FEM). For wave propagation problems wherein the frequency content of the input is very high, many higher order vibrational modes participate in the motion. At these higher frequencies, the wavelengths are very small and hence to capture these modes effectively, FE meshes need to be very fine. This is due to the requirement that the element sizes should be of the same order as the wavelength of the signal. For larger mesh sizes, the element edges will act like a free boundary and start reflecting the initial

responses from these element edges. A fine mesh, although ensuring accurate distribution of the inertia, also increases the computation cost enormously.

FE solutions in dynamics are obtained by two different methods [1]; the modal method and the time marching scheme. Modal methods cannot be applied to multi-modal problems such as those involving wave propagation analysis. This is because, unlike structural dynamics problems, here we need to determine the natural frequencies and the mode shapes of both the low and high frequency modes. It is well known that the extraction of the eigenvalues is computationally the most expensive problem in mechanics. Hence, modal methods are not suited to wave propagation problems. Alternatively we can use various time marching schemes under the FE environment. In this method, analysis is performed over a small time step, which is a fraction of the total time for which the response histories are required. For some time marching schemes, a constraint is placed on the time step, and this, coupled with very large mesh sizes, makes the solution of wave propagation problems (under the FE environment) computationally prohibitive. Hence, we need alternative methods of solution.

Numerical methods such as FEM are based on some assumed solutions to the field variable (say displacement). This assumed solution for wave propagation problems gives large system sizes due to its inability to approximate the mass distribution accurately. Hence, we need to look for a method that approximates the mass accurately. This can happen only when the assumed solution satisfies the governing wave equations as closely as possible. If one is interested in solving the governing wave equation in the time domain, it is very difficult to assume a solution that satisfies the governing wave equation. Instead, one can ignore the inertial part of the wave equation, and solve the static part of the equation exactly and use this solution to obtain the stiffness and mass matrices. This procedure will ensure that the stiffness distribution is nearly exact while the mass distribution is still approximate. Elements developed by this method are called the ***Super Convergent Finite Element (SCFE)***, which are formulated for higher order rods, beams, box-beams and inhomogeneous beams [2, 3, 4, 5, 6]. According to Reference [7], the error introduced by approximating stiffness is much higher than the approximate mass distribution. Hence, one can expect SCFE to give a smaller system size for wave propagation problems than conventional FEM.

Alternatively, one can transform the governing wave equation to the frequency domain and try to solve it exactly. This is a far easier option since transformation to the frequency domain removes the time variable from the governing equation and introduces frequency as a parameter. For 1-D systems, the transform method reduces a governing partial differential equation(s) to a set of ordinary differential equation(s), which are easier to solve than the original wave equation in the time domain. There are different transforms that one can use for this purpose, namely the *Laplace Transform*, the *Fourier Transform* and the *Wavelet Transform*. In this method first the wave equation is transformed into the frequency domain using appropriate forward transforms.

The governing equation in the transformed domain is then solved exactly or almost exactly and the results are post-processed to get all the relevant parameters in the frequency domain. The time domain solutions are then obtained by taking an inverse transform on the frequency domain solutions. Two aspects are very clear from the above discussion: (1) transform methods will yield solutions both in the time and the frequency domain; (2) one requires an efficient way of obtaining inverse transforms, either analytically or numerically, to obtain time domain solutions. If we look at the various available transforms, obtaining inverse Laplace transforms is not straightforward in most cases and this has limited its scope in the analysis of wave propagation problems. On the other hand, numerical versions of forward and inverse transforms are available for both the Fourier and Wavelet Transforms. The Fourier Transform uses the *Fast Fourier Transform* (FFT) numerical algorithm, while in the case of the Wavelet Transform, the Daubechies wavelet basis is commonly used for approximation in time. However, the Fourier transform is the most extensively used transform method for the solution of wave propagation problems due to its numerical superiority and the ease of implementation of the FFT algorithm. The ***Spectral Finite Element Method*** (SFEM) is a numerical method evolved from the Fourier Transform based method. More details on the solution schemes are given in Section 3.4.

There are certain advantages that a transform method can offer over conventional FEM. Unlike the direct problem, wherein one determines the response to the given input, inverse problems deal with determining the input history using the measured responses or determining the system as a whole from the known input and output. These problems are called force (or source) identification problems and system identification problems, respectively. Using a transform method such as SFEM, one can perform inverse problems in a simple and straightforward manner. This is made possible due to an algebraic relationship between the output and the input through the system transfer function (frequency response function). In other words, the transform methods can give responses in both the time and frequency domain using a single analysis.

The SFEM was initially conceived by Narayan and Beskos [8]. This was later popularized by Doyle and co-workers [9]. In recent years, there has been an increasing number of papers on this method in the archival literature for various structural applications. Although its application to metallic structures is well documented, its application to the study of wave propagation in anisotropic and inhomogeneous structures is not well reported in the literature. Unlike metallic structures, the wave behavior in anisotropic and inhomogeneous structures is quite complex due to the presence of both stiffness and inertial coupling. These couplings sometimes give rise to newer set of waves. In addition, the SFEM has potential for use in the application of ***Structural Health Monitoring***(SHM) and ***Active Wave Control*** (AWC), since both these problems involve loading having a very high frequency content. Hence, the main objective of this book is to bring out the essential wave characteris-

tics in these complex structures and show how SHM and AWC problems can be effectively handled in the SFEM environment.

Studies involving the monitoring, detection and arrest of the growth of flaws such as cracks constitute what is universally termed Structural Health Monitoring (SHM). SHM is a type of inverse problem, wherein the presence of damage needs to be detected from the known input and the measured output. It is well known that the most common method of detecting damage is through modal methods [10], wherein one can look at the changes in the natural frequencies of the structure before and after the damage to assess/confirm the presence of damage. In laminated composites, the most common form of failure is the delamination of the plies. At the onset of the damage, the stiffness of the structure reduces, but this reduction is negligible for very small size damage. Hence, modal methods will show negligible change in the lower energy modes and higher modes may become slightly perturbed. The computational cost of determining the higher modes limits the use of modal methods for SHM of composite structures. In summary, small size damage affects only the higher order modes leaving the lower modes unchanged. This effectively means that to assess the presence of small size damage, one needs a mathematical model that can capture the high frequency response of the damaged structure with small problem sizes. In other words, we need a wave propagation based diagnostic tool for SHM studies. This is one of the fundamental goals of on-line SHM, and the SFEM is an ideal candidate for this kind of analysis.

The main requirements for on-line SHM are the following:

- Mathematical models to represent various types of damage. Some of the common types of damage in laminated composites are delamination (both single and multiple), fibre breakage, and surface breaking cracks. Also, models are required for aging composite structures with degraded properties. One can easily model all types of damage using the conventional FEM using 2-D or 3-D elements. The singularity near the flaw tip requires fine mesh discretization. In addition, the high frequency loading requirement for SHM studies further increases the mesh density. These obviously increase the time for solution, defeating the very purpose of on-line SHM. In this book, we describe simplified but accurate spectral element models for various types of damage for its use in SHM studies.
- Accurate damage detection algorithms that blend with the mathematical model used to represent the damage. The success of a damage detection algorithm depends on the quality of the measured responses. Often these responses may be incomplete and in most cases they are corrupted by the presence of high frequency noise. The main requirement is that these damage detection algorithms should be able to predict the presence of damage in an uncertain environment.
- Robust sensors and their placement. The sensitivity of the sensor is an extremely important parameter that determines the quality of the measured

response. The sensitivity depends on the type of sensor and its placement with respect to the damage location. Smart sensors made from *Piezoceramics* (say lead-zirconate-titanate (PZT) or Polyvinylidene Difluoride (PVDF)) are extremely popular for SHM applications. Sensors made from magnetostrictive materials (say TERFENOL-D) are also quite popular due to their large free strain property. Surface Acoustic Wave (SAW) and Bulk Acoustic Wave (BAW) devices also find usage in SHM applications. The placement of the sensors is critical for accurate damage estimation. Normally, sensors are placed in regions of high stress, which are likely locations for damage initiation. However, these locations are difficult to determine *a priori*. Hence, the damage detection algorithm must be able to predict the location of the damage from the far field responses.

Active wave control is yet another application that deals with inputs that have high frequency content. Hence, SFEM is again a suitable candidate for such applications. Vibration reduction in a structure can normally be achieved passively by identifying the resonant conditions and suitably modifying the geometry of the structure such that the natural frequency of the system is far away from the driving frequency of the system. Alternatively, one can do a detailed analysis and identify the regions in a structure having high vibration levels and design suitable damping mechanisms to alleviate vibrations. However, design constraints may not allow any modification to the existing structure. These exercises can be undertaken only when the frequency content of the exciting force is small and when it is desired to reduce the modal amplitudes of the first few modes. Alternatively, one can design a feed back control system, for which an interrogating signal triggered at a certain frequency is required. This signal can be generated using smart actuators made from materials such as PZT, TERFENOL-D *et al.* However, the design of the control system poses a big problem if the problem sizes are large, as in the case of conventional FEM. In such cases, one has resort to reduced-order models for a given FE discretization. The fundamental requirement of any reduced-order model is that the high energy mode that requires suppression should be retained in the reduced model. This is a very difficult problem and requires an experienced analyst to choose the appropriate degrees of freedom to be retained in the reduced-order model. If the problem is a multi-modal one where all the higher modes also have significant energy, the FE discretization is also enormously large and hence to design a feedback control system for such problems, a reduced-order model of the structure is an absolute necessity. Again here, the choice of appropriate degrees of freedom to be included in the reduced-order model is more difficult than the earlier case. The SFEM, due to its inherent property of retaining all modal information within its small size, can effectively be used in multi-modal wave control. The SFEM does not require any reduced-order modelling and it can be used effectively with smart actuators for control applications.

1.2 Fourier Analysis

The heart of SFEM lies in the synthesis of waves using the Fourier transform. A time signal can be represented in the Fourier (frequency) domain in three possible ways, namely the *Continuous Fourier Transform*(CFT), the *Fourier Series* (FS) and the *Discrete Fourier Transform* (DFT). In this section, only brief definitions of the above transforms are given. The reader is encouraged to refer to [9] for more details.

1.2.1 Continuous Fourier Transforms

Consider any time signal $F(t)$. The inverse and the forward CFTs, normally referred to as the transform pair, are given by

$$F(t) = \frac{1}{2\pi} \int_{-\infty}^{\infty} \hat{F}(\omega) e^{j\omega t} d\omega, \quad \hat{F}(\omega) = \int_{-\infty}^{\infty} F(t) e^{-j\omega t} dt\,, \tag{1.1}$$

where $\hat{F}(\omega)$ is the CFT of the time signal, ω is the angular frequency and j ($j^2 = -1$) is the complex number. $\hat{F}(\omega)$ is necessarily complex and a plot of the amplitude of this function against frequency will give the frequency content of the time signal. As an example, consider a rectangular time signal of pulse width d. Mathematically, this function can be represented as

$$\begin{aligned} F(t) &= F_0 \qquad -d/2 \le t \le d/2 \\ &= 0 \qquad \text{otherwise}\,. \end{aligned} \tag{1.2}$$

This time signal is symmetrical about the origin. If this expression is substituted in Equation (1.1), we get

$$\hat{F}(\omega) = F_0 d \left\{ \frac{\sin(\omega d/2)}{\omega d/2} \right\}. \tag{1.3}$$

The CFT for this function is real only and symmetric about $\omega = 0$. The term inside the curly brace is called the *sinc* function. Also, the value of the CFT at $\omega = 0$ is equal to the area under the time signal.

Now the pulse is allowed to propagate in the time domain by an amount t_0 seconds. Mathematically such a signal can be written as

$$\begin{aligned} F(t) &= F_0 \qquad t_0 \le t \le t_0 + d \\ &= 0 \qquad \text{otherwise.} \end{aligned} \tag{1.4}$$

Substituting the above function in Equation (1.1) and integrating, we get

$$\hat{F}(\omega) = F_0 d \left\{ \frac{\sin(\omega d/2)}{\omega d/2} \right\} e^{-j\omega(t_0 + d/2)}\,. \tag{1.5}$$

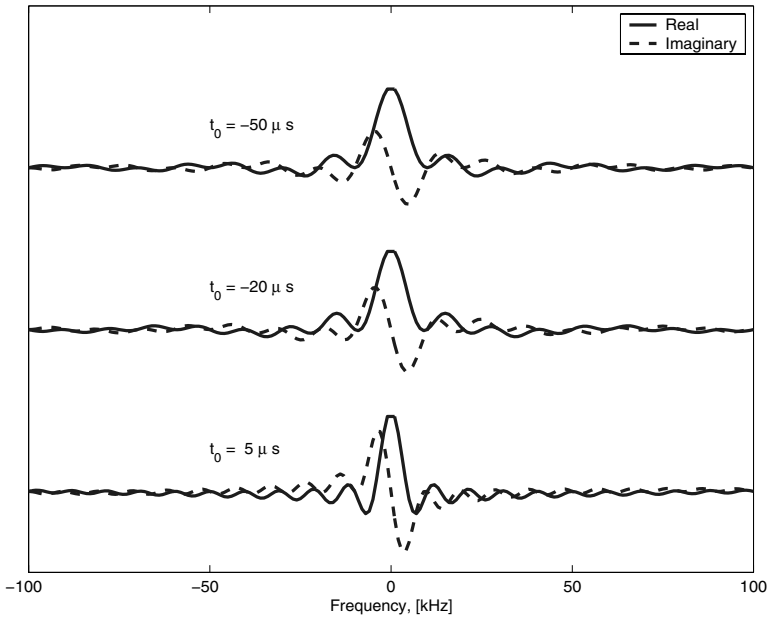

Fig. 1.1. Continuous Fourier transforms for various pulse width

The above CFT has both real and imaginary parts. These are also plotted in Figure 1.1. From Equations (1.3) and (1.5), we see that the magnitude of both these transforms are the same, however, the second transform has phase information built into it. Further, we see that the propagation of the signal in the time domain is associated with the change of phase in the frequency domain. Wave propagation problems are always associated with phase changes, which occur as the signal propagates. Based on the CFT, one can also determine the spread of the signal in both the time and frequency domain. For this, one has to look at the frequencies at which the CFT is zero. This occurs when

$$\sin\left(\frac{\omega_n d}{2}\right) = 0, \quad \text{or } \frac{\omega_n d}{2} = n\pi\,, \quad \text{or} \quad \omega_n = \frac{2n\pi}{d}\,,$$

$$\omega_2 - \omega_1 = \Delta\omega = \frac{4\pi}{d}\,.$$

That is, if the spread of the signal in the time domain is d then the spread in the frequency domain is $\Delta\omega = 4\pi/d$. Here, $\Delta\omega$ represents the frequency bandwidth. Hence, a Dirac delta function, which has infinitesimal width in the time domain, will have infinite bandwidth in the frequency domain. This aspect has greater implications in choosing the mesh sizes, when one resorts to FEM to solve the wave propagation problem. Following are some of the properties of the CFT:

- **Linearity:** Consider two time functions $F_1(t)$ and $F_2(t)$. The CFTs of these functions are given by $\hat{F}_1(\omega)$ and $\hat{F}_2(\omega)$, then the Fourier transform of the combined function is $F_1(t)+F_2(t) \Leftrightarrow \hat{F}_1(\omega)+\hat{F}_2(\omega)$. Here, the symbol $\Leftrightarrow$ is used to denote the CFT of a time signal. **Implications for wave propagation:** Here, $F_1(t)$ and $F_2(t)$ can be thought of as the incident and the reflected waves, respectively. The linearity property states that the combined transform of the incident and the reflected waves are equal to the individual transform of these obtained separately.
- **Scaling:** If a time signal is multiplied by a factor k to become $F(kt)$, the CFT of this time signal is given by $F(kt) \Leftrightarrow 1/k\hat{F}\,(\omega/k)$ **Implications for wave propagation:** Time domain compression is frequency domain expansion. This property fixes the frequency bandwidth of the given time signal.
- **Time shifting:** If a given time signal $F(t)$ is shifted by an amount t_s to become $F(t-t_s)$, the CFT of the shifted signal is given by $F(t-t_s) \Leftrightarrow \hat{F}(\omega)e^{-j\omega t}$. **Implications for wave propagation:** Propagation in the time domain is accompanied by phase changes in the frequency domain.
- **CFT is always complex:** Any given time function $F(t)$ can be split up into symmetric and anti-symmetric functions $F_s(t)$ and $F_a(t)$. Further, using the property of the linearity of the CFT, we can show that $F_s(t) = Real(\hat{F}(\omega))$ and $F_a(t) = jImag(\hat{F}(\omega))$. **Implications for wave propagation:** Since the time signals encountered in wave mechanics is neither symmetric (even) nor anti-symmetric in nature, the CFT is necessarily complex in nature. Hence, wave propagation problems are always associated with phase changes.
- **Symmetric property of the CFT:** Since the CFT of a time signal $F(t)$ is complex, it can be split into real and imaginary parts as $\hat{F}(\omega) = \hat{F_R}(\omega) + j\hat{F_R}I(\omega)$. Substituting this into the first part of Equation (1.1) and expanding the complex exponential in terms of the sine and cosine functions, we can write real and imaginary parts of the transform as

$$\hat{F}_R = \int_{-\infty}^{\infty} F(t)\cos(\omega t)dt, \quad \hat{F}_I = \int_{-\infty}^{\infty} F(t)\sin(\omega t)dt\,.$$

  The first integral is an even function and the second is an odd function, that is $\hat{F_R}(\omega) = \hat{F_R}(-\omega)$, and $\hat{F_I}(\omega) = -\hat{F_I}(-\omega)$. Now, if we consider the CFT about a point $\omega = 0$(origin), the transform on the right of the origin can be written as $\hat{F}(\omega) = \hat{F_R}(\omega) + j\hat{F_I}(\omega)$. Similarly, the transform to the left of the origin can be written as $\hat{F}(-\omega) = \hat{F_R}(-\omega)+j\hat{F_I}(-\omega) = \hat{F_R}(\omega)-j\hat{F_I}(\omega) = \hat{F}^*(\omega)$, which is the complex conjugate of the transform on the right side of the origin. The frequency point about which this happens is called the Nyquist frequency. **Implications for wave propagation:** The Nyquist frequency is an important parameter in wave propagation analysis, especially in the context of using the FFT (to be introduced later), since the analysis will be performed only up to this frequency.

- **Convolution:** This is a property relating to the product of two time signals $F_1(t)$ and $F_2(t)$. The CFT of the product of these two functions can be written as

$$\hat{F}_{12}(\omega) = \int_{-\infty}^{\infty} F_1(t)F_2(t)e^{-j\omega t}dt\,.$$

Substituting Equation (1.1) for both these functions in the above equation, we can write

$$\hat{F}_{12}(\omega) = \int_{-\infty}^{\infty} \hat{F}_1(\bar{\omega}) \int_{-\infty}^{\infty} F_2(t)e^{-j(\omega-\bar{\omega})t}dtd\bar{\omega} = \int_{-\infty}^{\infty} \hat{F}_1(\bar{\omega})\hat{F}_2(\omega-\bar{\omega})d\bar{\omega}$$

or

$$F_1(t)F_2(t) \Leftrightarrow \int_{-\infty}^{\infty} \hat{F}_1(\bar{\omega})\hat{F}_2(\omega-\bar{\omega})d\bar{\omega}\,.$$

The above form of CFT is called the convolution. Conversely, we can also write

$$\hat{F}_1(\omega)\hat{F}_2(\omega) \Leftrightarrow \int_{-\infty}^{\infty} F_1(\tau)F_2(t-\tau)d\tau\,.$$

Implication for wave propagation: The first property, using the product of two time domain signals, has its use in understanding signal processing aspects. For example, a truncated signal in the time domain is equal to the product of the original signal and the truncated signal. The second (or the converse) property is of great importance in wave propagation analysis. That is, all the responses (outputs) of a mechanical waveguide to applied loadings can be represented as the frequency domain product of the input and the system transfer function. Thus the time responses are obtained by convolving the transfer functions with the load spectrum.

1.2.2 Fourier Series

Both the forward and the inverse CFT require mathematical description of the time signal as well as their integration. In most cases, the time signals are point data acquired during experimentation. Hence, what we require is the numerical representation for the transform pair (Equation (1.1)), which is called the Discrete Fourier Transform (DFT). The DFT is introduced in detail in the next subsection. The Fourier Series (FS) is in between the CFT and the DFT, wherein the inverse transform is represented by a series, while the forward transform is still in the integral form as in CFT. That is, one still needs the mathematical description of the time signal to obtain the transforms.

The FS of a given time signal can be represented as

$$F(t) = \frac{a_0}{2} + \sum_{n=1}^{\infty} \left[a_n \cos\left(2\pi n \frac{t}{T}\right) + b_n \sin\left(2\pi n \frac{t}{T}\right) \right] \tag{1.6}$$

where $(n = 0, 1, 2, \ldots)$

$$a_n = \frac{2}{T} \int_0^T F(t) \cos\left(\frac{2\pi n t}{T}\right) dt, \quad b_n = \frac{2}{T} \int_0^T F(t) \sin\left(\frac{2\pi n t}{T}\right) dt. \tag{1.7}$$

Equation (1.6) corresponds to the inverse transform of the CFT, while Equation (1.7) corresponds to the forward transforms of the CFT. Here T is the period of the time signal, *i.e.,* the discrete representation of a continuous time signal $F(t)$, introduces periodicity of the time signal. The FS given in Equation (1.6) can also be written in terms of complex exponentials, which can give one-to-one comparison with CFT. That is, Equations (1.6) and (1.7) can be rewritten as

$$\begin{aligned} F(t) &= \tfrac{1}{2} \sum_{-\infty}^{\infty} (a_n - b_n) e^{j\omega_n t} = \sum_{-\infty}^{\infty} \hat{F}_n e^{j\omega_n t}, \quad n = 0, \pm 1, \pm 2, \ldots \\ \hat{F}_n &= \tfrac{1}{2}(a_n - b_n) = \tfrac{1}{T} \int_0^T F(t) e^{-j\omega_n t} dt, \;, \;\; \omega_n = \tfrac{2\pi n}{T}. \end{aligned} \tag{1.8}$$

Because of enforced periodicity, the signal repeats itself after every T seconds. Hence, we can define the fundamental frequency either in radians per second (ω_0) or Hz $(f_0 = \omega_0/2\pi = 1/T)$. We can now express the time signal in terms of the fundamental frequency as

$$F(t) = \sum_{-\infty}^{\infty} \hat{F}_n e^{j2\pi n f_0 t} = \sum_{-\infty}^{\infty} \hat{F}_n e^{jn\omega_0 t}. \tag{1.9}$$

From Equation (1.9), it is clear that, unlike in CFT, the transform given by FS is discrete in frequency. To understand the behavior of FS as opposed to the CFT, the same rectangular time signal used earlier is again considered here. The FS coefficients (or transform) are obtained by substituting the time signal variation in Equation (1.8). This is given by

$$\hat{F}_n = \frac{F_0}{T} \left[\frac{\sin(n\pi d/T)}{(n\pi d/T)} \right] e^{-j(t_0 + d/2)2\pi n/T}. \tag{1.10}$$

The plot of the transform amplitude obtained from the CFT and the FS are shown in Figure 1.2. The figure shows that the values of the transform obtained by FS at discrete frequencies fall exactly on the transform obtained by CFT. The figure also shows the transform values for different time periods T. We see from the figure that the larger the time period, the closer are the frequency spacings. Hence, if the period tends to infinity, the transform obtained by FS will be exactly equal to the transform obtained by CFT.

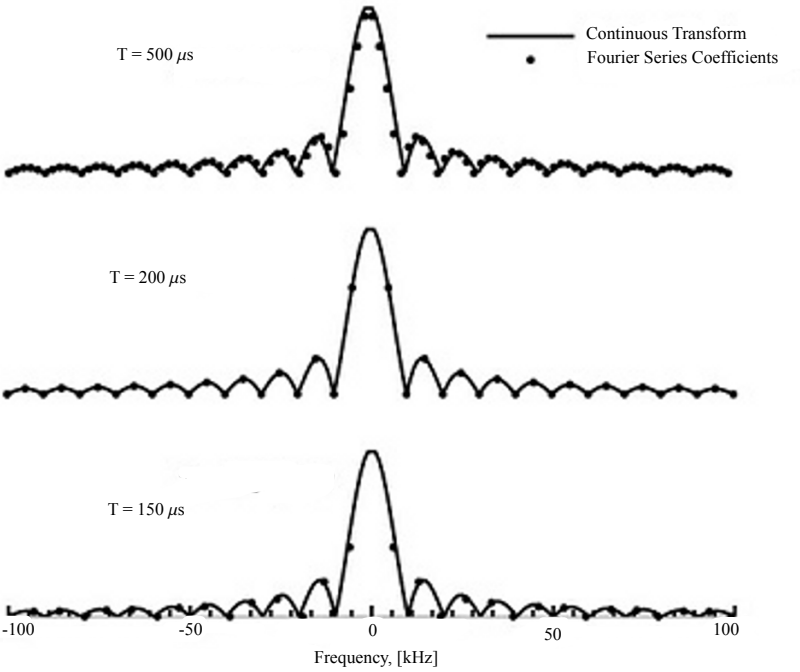

Fig. 1.2. Comparison of Fourier series with Continuous Fourier Transforms

1.2.3 Discrete Fourier Transform

The Discrete Fourier transform (DFT) is an alternative way of mathematically representing the CFT in terms of summations. Here, both the forward and inverse CFT given in Equation (1.1) are represented by summations. This will completely do away with all complex integration involved in the computation of CFT. In addition, it is not necessary to represent the time signals mathematically and the great advantage of this is that one can use the time data obtained from experiment. Numerical implementation of the DFT is done using the famous FFT algorithm.

We begin here with Equation (1.8), which is the FS representation of the time signal. The main objective here is to replace the integral involved in the computation of the Fourier coefficients by summation. For this, the plot of time signal shown in Figure 1.3 is considered.

The time signal is divided into M piecewise constant rectangles, whose height is given by F_m, and the width of these rectangles is equal to $\Delta T = T/M$. We derived earlier that the continuous transform of a rectangle is a *sinc* function. By rectangular idealization of the signal, the DFT of the signal will be the summation of M *sinc* functions of pulse width ΔT and hence the second integral in Equation (1.8) can now be written as

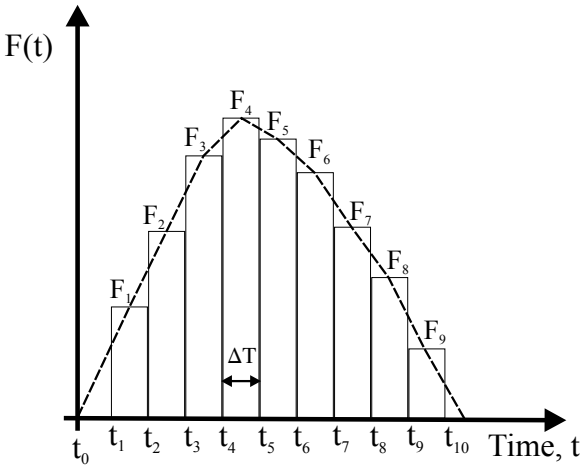

Fig. 1.3. Time signal discretization for DFT

$$\hat{F}_n = \Delta T \left[\frac{\sin(\omega_n \Delta T/2)}{(\omega_n \Delta T/2)} \right] \sum_{m=0}^{M} F_m e^{-j\omega_n t_m} \tag{1.11}$$

Let us now look at the *sinc* function in Equation (1.11). Its value depends on the width of the rectangle ΔT. That is, as the width of the rectangle becomes smaller, the term inside the bracket of Equation (1.11) tends to unity value. This will happen for all values of $n < M$. It can easily be shown that for values of $n \geq M$, the values of the transform is approximately equal to zero. Hence, the DFT transform pairs can now be written as

$$\begin{aligned} F_m &= F(t_m) = \tfrac{1}{T} \sum_{n=0}^{N-1} \hat{F}_m e^{j\omega_n t_m} = \tfrac{1}{T} \sum_{n=0}^{N-1} \hat{F}_m e^{j2\pi nm/N} \\ \hat{F}_n &= \hat{F}(\omega_n) = \Delta T \sum_{n=0}^{N-1} F_m e^{-j\omega_n t_m} = \Delta T \sum_{n=0}^{N-1} F_m e^{-j2\pi nm/N} \end{aligned} \tag{1.12}$$

Here, both m and n range from 0 to N−1.

The periodicity of the time signal is necessary for DFT as we begin from the FS representation of the time signal. Now, we can probe a little further to see whether the signal has any periodicity in the frequency domain. For this, we can look at the summation term in Equation (1.11). Hypothetically, let us assume $n > M$. Hence, we can write $n = M + \bar{n}$. Then, the exponential term in the equation becomes

$$e^{-j\omega_n t_m} = e^{-jn\omega_0 t_m} = e^{-jM\omega_0 t_m} e^{-j\bar{n}\omega_0 t_m} = e^{-j2\pi m} e^{-j\bar{n}\omega_0 t_m} = e^{-j\bar{n}\omega_0 t_m} .$$

Hence, the summation term in Equation (1.11) becomes

$$\Delta T \sum_{m=0}^{M-1} F_m e^{-j\bar{n}\omega_0 t_m} .$$

This term shows that the above summation has the same value when $n = \bar{n}$. For example, if $M = 6$, then the value of the summation for $n = 9, 11, 17$ is same as the value for $n = 3$, 5, and 11 respectively. Two aspects are very clear from this analysis. First, $n > M$ is not important, and second, there is forced periodicity in both the time and frequency domain in using DFT. This periodicity occurs about a frequency where the transform goes to zero. This frequency can be obtained if one looks at the *sinc* function given in Equation (1.11). That is, the argument of the *sinc* function is given by

$$\frac{\omega_n \Delta T}{2} = \pi n \Delta T = \frac{\pi n}{M}$$

where, we have used the relation $\Delta T = T/M$.

Here, we see that the *sinc* function goes to zero when $n = M$. It is at this value of n that the periodicity is enforced and the frequency corresponding to this value is called the *Nyquist* frequency. As mentioned earlier, this happens due to the time signal being real only and the transform beyond the Nyquist frequency is the complex conjugate of the transform before this frequency. Thus, N real points are transformed to $N/2$ complex points. Knowing the sampling rate ΔT, we can compute the Nyquist frequency from the expression

$$f_{Nyquist} = \frac{1}{2\Delta T} . \tag{1.13}$$

There are a number of issues in the numerical implementation of the DFT, which are not discussed here. However, the reader is encouraged to consult Reference [9] to get more information on these aspects. In all the wave propagation examples given in this textbook, the FFT is used to transform the signal back and forth from the time and frequency domains and vice versa. In order to see the difference in different transform representation, the same rectangular pulse is again used here. There are two parameters on which the accuracy of the transforms obtained by the DFT depends, namely the sampling rate ΔT and the time window parameter N. Figures 1.4 and 1.5 show the transform obtained for various sampling rates ΔT and time window parameter N. From the figures, we can clearly see the periodicity about the Nyquist frequency. For a given time window N, the figure shows that the frequency spacing increases with decreasing sampling rate. Also, the Nyquist frequency shifts to a higher value. Next, for a given sampling rate ΔT, the time window is varied through the parameter N. In this case, the Nyquist frequency does not change. However, for larger N, the frequency spacing becomes smaller and hence we get denser frequency distribution.

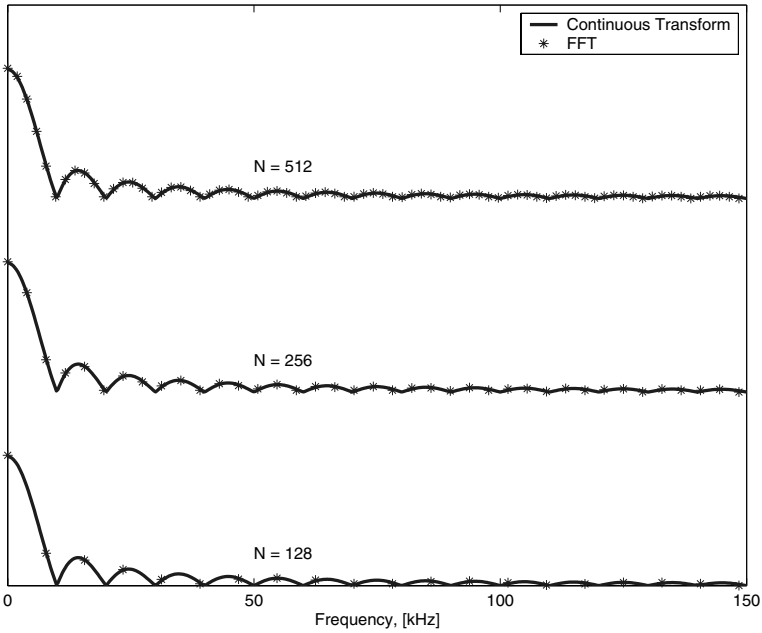

Fig. 1.4. Comparison of FFT and continuous transform for a sampling rate $\Delta T = 1\mu s$

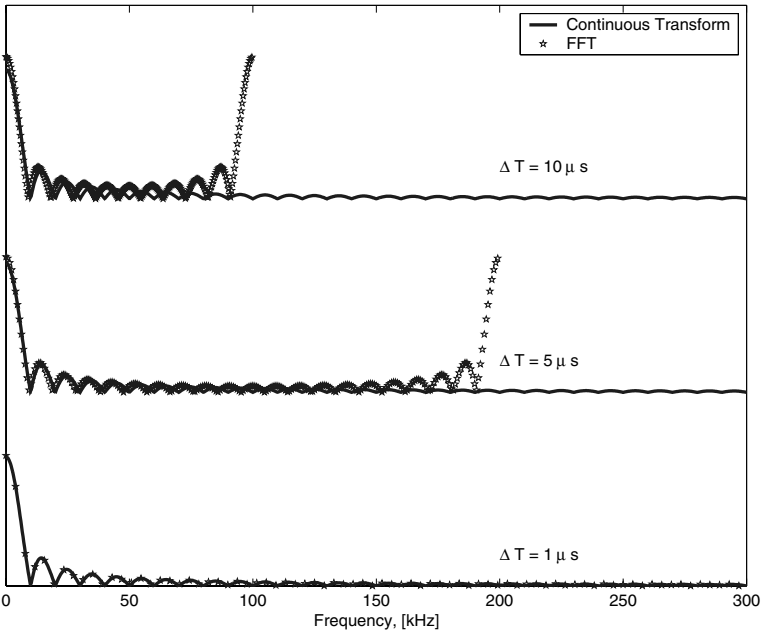

Fig. 1.5. Comparison of FFT and continuous transform for different sampling rates

1.3 Spectral Analysis

SFEM uses spectral analysis to obtain the local wave behavior for different waveguides and hence the wave characteristics, namely the *Spectrum* and the *Dispersion* relation. These local characteristics are synthesized to get the global wave behavior. Spectral analysis uses DFT to represent a field variable (say displacement) as a finite series involving a set of coefficients, which requires to be determined based on the boundary conditions of the problem. Spectral analysis enables the determination of two important wave parameters, namely the *wavenumbers* and the *group speeds*. These parameters are not only required for spectral element formulation, but also to understand the wave mechanics in a given waveguide. These parameters enable us to know whether the wave mode is a propagating mode or a damping mode or a combination of these two (propagation as well as wave amplitude attenuation). If the wave is propagating, the wavenumber expression will let us know whether it is *non-dispersive* (that is, the wave retains its shape as it propagates) or *dispersive* (when the wave changes its shape as it propagates). In this section, for the sake of completeness, we give a brief outline of spectral analysis for second- and fourth-order systems. More details can be found in Reference [9].

The starting point of spectral analysis is the governing differential equation. Consider a second-order partial differential equation given by

$$a\frac{\partial^2 u}{\partial x^2} + b\frac{\partial u}{\partial x} = c\frac{\partial^2 u}{\partial t^2} \tag{1.14}$$

where, *a, b, c* are known constants and $u(x,t)$ is the field variable, x is the spatial variable and t is the temporal variable. We first approximate or transform the above partial differential equation (PDE) to the frequency domain using DFT, which is given by

$$u(x,t) = \sum_{n=0}^{N-1} \hat{u}_n(x,\omega_n)e^{j\omega_n t} \tag{1.15}$$

where, ω_n is the circular frequency and N is the total number of frequency points used in the approximation. Here $\hat{u}$ is the frequency-dependent Fourier transform of the field variable. Substituting Equation (1.15) into Equation (1.14), we get

$$a\frac{d^2\hat{u}_n}{dx^2} + b\frac{d\hat{u}_n}{dx} + c\omega_n^2\hat{u}_n = 0\,, n = 0,\ldots,N-1\,. \tag{1.16}$$

From the above equation, we see that a partial differential equation is reduced to a set of ordinary differential equation (ODE) with the time variation removed and instead, the frequency introduced as a parameter. The summation is omitted in the above equation for brevity. Equation (1.16) is a constant coefficient ODE, which has a solution of the type $\hat{u}_n(x,\omega) = A_n e^{jkx}$, where A_n

is some unknown constant and k is called the *wavenumber*. Substituting the above solution in Equation (1.16), we get the following characteristic equation to determine k

$$(k^2 - \frac{bj}{a}k + \frac{c\omega_n^2}{a})A_n = 0\,. \tag{1.17}$$

The above equation is quadratic in k and has two roots corresponding to the two modes of wave propagation. These two modes correspond to the incident and reflected waves. If the wavenumbers are real, then the wave modes are called *propagating modes*. On the other hand, if the wavenumbers are complex, then the wave modes damp out the responses and hence they are called *evanescent modes*. These are given by

$$k_{1,2} = \frac{bj}{2a} \pm \sqrt{\frac{-b^2}{4a^2} + \frac{c\omega_n^2}{a}}\,. \tag{1.18}$$

Equation (1.18) is the generalized expression for the determination of the wavenumbers. Different wave behavior is possible depending upon the values of $a, b,$ and c. The behavior also depends on the numerical value of the radical $\sqrt{c\omega_n^2/a - b^2/4a^2}$. Let us consider a simple case of $b = 0$. The two wavenumbers are given by

$$k_1 = \omega_n \frac{c}{a}, \qquad k_2 = -\omega_n \frac{c}{a}\,. \tag{1.19}$$

From the above expression, we find that the wavenumbers are real and hence they are propagating modes. The wavenumbers are linear functions of frequency ω. At this point, we would like to introduce two important wave parameters that will determine the wave characteristics, namely the ***phase speed*** C_p and ***group Speed*** C_g. They are defined as

$$C_p = \frac{\omega_n}{Real(k)}, \qquad C_g = \frac{d\omega_n}{dk}\,. \tag{1.20}$$

For the wavenumbers given in Equation (1.19), the speeds are given by

$$C_p = C_g = \frac{a}{c}\,. \tag{1.21}$$

We find that both group and phase speed are constant and equal. Hence, when wavenumbers vary linearly with frequency ω and phase speed and group speed are constant and equal, then the wave, as it propagates, retains its shape. Such waves are called ***Non-dispersive waves***. Longitudinal waves in elementary rods are of this type. If the wavenumber varies in a non-linear manner with respect to the frequency, the phase and group speeds will not be constant but will be functions of frequency ω. That is, each frequency component travels with different speed and as a result, the wave changes its shape as it propagates. Such waves are called ***dispersive waves***.

Next, let us again consider Equation (1.18) with all the constants nonzero. The wavenumber no longer varies linearly with the frequency. Hence, one can expect dispersive behavior of the waves and the level of dispersion will depend upon the numerical value of the radical. We will investigate this aspect in a little more detail. There can be the following three situations:

1. $b^2/4a^2 > c\omega_n^2/a$
2. $b^2/4a^2 < c\omega_n^2/a$ and
3. $b^2/4a^2 = c\omega_n^2/a$

Let us now consider Case 1. When $(b^2)/(4a^2) > (c\omega_n^2)/(a)$, then the radical will be a complex number and hence all the wavenumbers will be complex, implying that the wave modes are not propagating and they would damp out rapidly. For Case 2, where $(b^2)/(4a^2) < (c\omega_n^2)/(a)$, the value of the radical will be positive and real and hence the wavenumber will have both real and imaginary parts, *i.e.*,, takes the form $k = p + jq$. Hence, waves having this feature will attenuate as they propagate. The phase and group speeds for this case are given by

$$C_p = \frac{\omega_n}{k} = \frac{\omega_n}{\sqrt{c\omega_n^2/a - b^2/4a^2}}\,, \tag{1.22}$$

$$C_g = \frac{d\omega_n}{dk} = \frac{a\sqrt{c\omega_n^2/a - b^2/4a^2}}{c\omega_n}\,. \tag{1.23}$$

It is quite obvious that these are not the same and hence the waves could be dispersive in nature. One can get back the non-dispersive solution by substituting $b = 0$ in Equation (1.23). Now, let us see Case 3 where the value of the radical will be zero and hence the wavenumber is purely imaginary indicating that the wave mode is a damping mode. The interesting point here is to find the frequency of transition at which the propagating mode becomes evanescent or a damping mode. This can be obtained by equating the radical to zero. Thus the transition frequency ω_t is given by

$$\omega_t = \frac{b}{2\sqrt{ac}}\,.$$

Once the wavenumbers are determined, the solution to the governing wave equation (Equation (1.16)) in the frequency domain can be written as (for $b = 0$)

$$\hat{u_n}(x, \omega_n) = A_n e^{-jk_n x} + B_n e^{jk_n x}, \qquad k_n = \omega_n \sqrt{\frac{c}{a}}\,. \tag{1.24}$$

In the above equation A_n represents the incident wave coefficient while B_n represents the reflected wave coefficient. Solution of the governing equation in the frequency domain is the starting point for the SFEM.

It is clearly seen how the values of the constants in the governing differential equation play an important part in dictating the type of wave propagation